

## Highly Efficient Detection and Separation of Chiral Molecules through Shortcuts to Adiabaticity

Nikolay V. Vitanov<sup>1</sup> and Michael Drewsen<sup>2</sup>

<sup>1</sup>*Department of Physics, St. Kliment Ohridski University of Sofia, James Bourchier 5 blvd, BG-1164 Sofia, Bulgaria*

<sup>2</sup>*Department of Physics and Astronomy, Aarhus University, DK-8000 Aarhus C, Denmark*



(Received 29 January 2019; published 3 May 2019)

A highly efficient method for optical or microwave detection and separation of left- and right-handed chiral molecules is proposed. The method utilizes a closed-loop three-state system in which the population dynamics depends on the phases of the three couplings. Because of the different signs of the coupling between two of the states for the opposite chiralities the population dynamics is chirality dependent. By using the “shortcuts to adiabaticity” concept applied to the stimulated Raman adiabatic passage technique, one can achieve 100% contrast between the two enantiomers in the population of a particular state. It can be probed by light-induced fluorescence for large ensembles or through resonantly enhanced multiphoton ionization for single molecules.

DOI: [10.1103/PhysRevLett.122.173202](https://doi.org/10.1103/PhysRevLett.122.173202)

**Introduction.**—Ever since its discovery by Pasteur in 1848 [1] chirality has played an important role in chemistry, biotechnologies, and pharmaceuticals due to its significance to living matter. Moreover, precise control of the rotational populations of chiral molecules opens a plethora of new possibilities, e.g., in studies of parity violation in chiral molecules [2,3]. Yet, the detection and separation of racemic mixtures of enantiomers, i.e., molecules with opposite left ( $L$ ) and right ( $R$ ) handedness, referred to as chiral resolution, is one of the outstanding challenges in chemistry [4]. Conventionally, it is achieved by sophisticated, time-consuming, and expensive chemical techniques, e.g., crystallization, derivatization, kinetic resolution, and chiral chromatography [5].

As an alternative, optical (termed “chiroptical”) methods offer some promising features. They use the fact that the mirror symmetry of enantiomers can be broken using circularly polarized electromagnetic fields [6]. Well-established chiroptical methods include optical rotary dispersion [6], circular dichroism [7] (e.g., vibrational [8,9] and photoelectron [10–12]), and Raman optical activity [8,13]. Circularly polarized light interacts with chiral molecules via the (weak) magnetic-dipole interaction [14,15]. Alternative methods for achieving enantioselectivity have been proposed with linearly polarized light that use the far stronger electric-dipole interaction with the field [16–21]. What makes chiral separation feasible in such schemes is the sign difference in some of the transition dipole moments of the  $L$  and  $R$  enantiomers (see Fig. 1), which can be mapped onto population difference by subjecting the chiral molecules to an appropriately timed and phased set of electromagnetic fields.

In a complementary approach, Shapiro *et al.* [22–29] proposed to detect and separate enantiomers by using

concepts from the adiabatic passage techniques [30], which offer robustness to various experimental errors. They considered a four-state closed-loop double- $\Lambda$  or diamond configuration [22–25], and a closed-loop three-state system driven by three delayed but overlapped laser fields ( $P$ ,  $S$ , and  $Q$ ) [26–29]; see Fig. 1. In addition, nonzero detunings are used, which generate avoided crossings between the adiabatic states. For  $L$  and  $R$  handedness, the avoided crossings occur between different adiabatic states, thereby driving the population evolution along different paths toward different final states.

While the laser-based schemes of Shapiro *et al.* have not been demonstrated yet, chiral resolution in the gas phase by electromagnetic fields has been demonstrated using chirality-sensitive microwave spectroscopy [31]. Here, three-wave mixing in a cooled gas cell or in a supersonic molecular beam [32–36] was combined with broadband chirped-pulse rotational spectroscopy [37,38]. Chiral separation can furthermore be achieved by applying three resonant pulsed fields with appropriate phases on all three

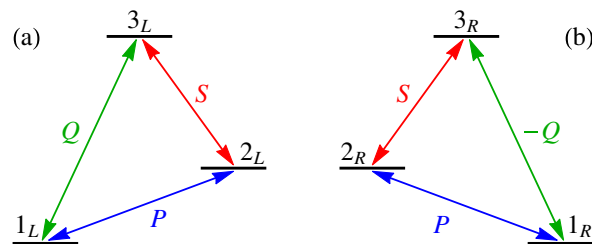


FIG. 1. Comparison of the coupling schemes between three discrete energy states in molecules with  $L$  (a) and  $R$  (b) handedness. The only difference is in the sign of the coupling  $Q$  on the transition  $|1\rangle \leftrightarrow |3\rangle$ .

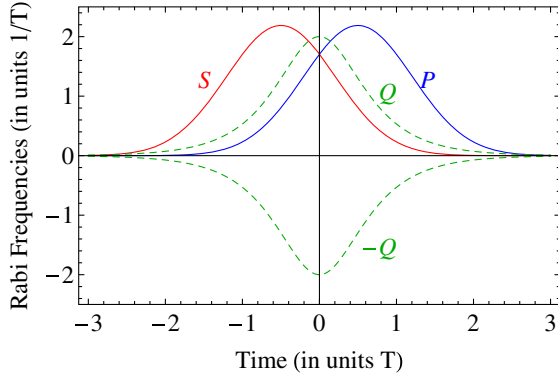


FIG. 2. Timing of the  $P$ ,  $S$ , and  $Q$  couplings for Gaussian pulse shapes of the  $P$  and  $S$  fields. The coupling  $Q$  has opposite signs for  $L$ - and  $R$ -handed molecules.

transitions which lead to different enantio-selective population distributions [39], as has been very recently demonstrated experimentally in both buffer gas cell [40] and supersonic expansion [41].

In this Letter, we follow the original idea of Shapiro *et al.* and propose a different scheme, which is simpler and faster, and its efficiency is essentially 100%. It still requires delayed pulses with some mutual overlap (see Fig. 2), but it works on resonance, and the required pulse areas are only of the order of  $\pi$ , which means that the scheme is very fast.

Our scheme combines the loop linkage of Shapiro *et al.* with an idea reminiscent to “shortcuts to adiabaticity.” It was first proposed by Bergmann and co-workers [42], who suggested to use the  $Q$  pulse to cancel the nonadiabatic coupling in the well-known and widely used technique of stimulated Raman adiabatic passage (STIRAP) and ensure perfect adiabaticity with moderate pulse areas. Similar ideas were proposed later by Demirplak and Rice [43] who used the term “counterdiabatic field,” and by Chen *et al.* [44] who nailed the very appealing term “shortcut to adiabaticity.”

*Physical mechanism.*—Because of its interferometric nature, the closed-loop scheme is phase sensitive. It is exactly this phase sensitivity which is used here to separate the two enantiomers because for them the overall phase in the loop linkage differs by  $\pi$ . The key idea of our scheme is that for one enantiomer, e.g.,  $L$ -handed, the  $Q$  field works as a shortcut to adiabaticity for it cancels the nonadiabatic coupling and induces perfect population transfer between states  $|1\rangle$  and  $|3\rangle$ , with probability  $P_{1\rightarrow 3} = 1$ . For the opposite  $R$  handedness, the same  $Q$  field acts oppositely due to the different sign of the coupling, and it doubles rather than cancels, the nonadiabatic coupling. For specific values of the pulse areas, the population transfer  $|1\rangle \rightarrow |3\rangle$  is canceled completely:  $P_{1\rightarrow 3} = 0$ . Therefore, the handedness is determined by measuring the population in state  $|3\rangle$  alone: 0 for one handedness and 1 for the opposite handedness.

We consider a three-state system in which all three transitions are driven simultaneously, thereby forming a phase-sensitive interferometric linkage pattern, as shown in Fig. 1. The Hamiltonian of this system reads

$$\mathbf{H}^{L,R} = \frac{1}{2} \begin{bmatrix} 0 & \Omega_p & \pm\Omega_q e^{i\phi} \\ \Omega_p^* & 0 & \Omega_s \\ \pm\Omega_q e^{-i\phi} & \Omega_s^* & 0 \end{bmatrix}, \quad (1)$$

where the superscripts  $L$  and  $R$  denote the handedness.  $\Omega_x(t)$  with  $x = p, s, q$  is the Rabi frequency quantifying the coupling for the  $P$ ,  $S$ , or  $Q$  transition. The only difference between  $L$  and  $R$  handedness is in the sign of the  $Q$  coupling, the  $+$  ( $-$ ) sign being for  $L$  ( $R$ ) handedness. The  $Q$  coupling has a phase  $\phi$ , which, following Ref. [42] will be set to  $\pi/2$ . Without loss of generality we assume hereafter that  $\Omega_p$ ,  $\Omega_s$ , and  $\Omega_q$  are real and positive.

First, let us assume that the  $Q$  coupling is zero, i.e.,

$$\mathbf{H}_0 = \frac{1}{2} \begin{bmatrix} 0 & \Omega_p & 0 \\ \Omega_p & 0 & \Omega_s \\ 0 & \Omega_s & 0 \end{bmatrix}. \quad (2)$$

The three eigenvalues of this Hamiltonian are  $\lambda_- = -\Omega$ ,  $\lambda_0 = 0$ ,  $\lambda_+ = \Omega$ , where  $\Omega = \sqrt{\Omega_p^2 + \Omega_s^2}$ . The corresponding eigenvectors of  $\mathbf{H}_0$  are

$$|\chi_-\rangle = \frac{\sin\theta|1\rangle - |2\rangle + \cos\theta|3\rangle}{\sqrt{2}}, \quad (3a)$$

$$|\chi_0\rangle = \cos\theta|1\rangle - \sin\theta|3\rangle, \quad (3b)$$

$$|\chi_+\rangle = \frac{\sin\theta|1\rangle + |2\rangle + \cos\theta|3\rangle}{\sqrt{2}}, \quad (3c)$$

with  $\tan\theta(t) = \Omega_p(t)/\Omega_s(t)$ . In STIRAP, the pump and Stokes pulses are delayed to each other, with the Stokes pulse coming first [30]. Therefore,  $\theta(t)$  changes from 0 initially to  $\pi/2$  in the end and hence the eigenstate  $|\chi_0\rangle$  behaves as state  $|1\rangle$  initially and state  $-|3\rangle$  at the end, thereby providing an adiabatic link between these two states. If the system starts in state  $|1\rangle$  initially and evolves adiabatically, then it will remain in the eigenstate  $|\chi_0\rangle$  at all times and will end up in state  $|3\rangle$ .

We use the eigenstates (3) to form the transformation matrix

$$\mathbf{W} = \begin{bmatrix} \frac{\sin\theta}{\sqrt{2}} & \cos\theta & \frac{\sin\theta}{\sqrt{2}} \\ -\frac{1}{\sqrt{2}} & 0 & \frac{1}{\sqrt{2}} \\ \frac{\cos\theta}{\sqrt{2}} & -\sin\theta & \frac{\cos\theta}{\sqrt{2}} \end{bmatrix}, \quad (4)$$

and we switch the  $Q$  coupling on. The full Hamiltonian (1)

(with  $\phi = \pi/2$ ) is transformed in the basis of the eigenstates (3) of  $\mathbf{H}_0$  as  $\mathbf{H}_a = \mathbf{W}^T \mathbf{H} \mathbf{W} - i \mathbf{W}^T \dot{\mathbf{W}}$  (note that  $\mathbf{W}^{-1} = \mathbf{W}^T$ ). Explicitly,

$$\mathbf{H}_a^{L,R} = \begin{bmatrix} -\frac{1}{2}\Omega & \frac{i}{\sqrt{2}}(\dot{\theta} \mp \frac{1}{2}\Omega_q) & 0 \\ -\frac{i}{\sqrt{2}}(\dot{\theta} \mp \frac{1}{2}\Omega_q) & 0 & -\frac{i}{\sqrt{2}}(\dot{\theta} \mp \frac{1}{2}\Omega_q) \\ 0 & \frac{i}{\sqrt{2}}(\dot{\theta} \mp \frac{1}{2}\Omega_q) & \frac{1}{2}\Omega \end{bmatrix}, \quad (5)$$

with the upper (lower) sign being for  $L$  ( $R$ ) handedness. Here the choice of the phase  $\pi/2$  of the  $Q$  coupling in Eq. (1) becomes clear: the  $Q$  coupling adds to, or subtracts from, the nonadiabatic coupling  $\dot{\theta}$ . We have achieved something very important: the sign difference in the couplings for the  $Q$  transition is mapped onto different magnitudes of the couplings between states  $|\chi_0\rangle \leftrightarrow |\chi_-\rangle$  and  $|\chi_0\rangle \leftrightarrow |\chi_+\rangle$ . It is this difference that is used here to distinguish the two enantiomers.

If we choose (see Fig. 2)

$$\Omega_q(t) = 2\dot{\theta}(t), \quad (6)$$

then the off-diagonal elements in  $\mathbf{H}_a^L$  will vanish and the system will be locked in its initial state  $|\chi_0\rangle$  as no transition in this basis can occur. On the contrary, the off-diagonal elements in  $\mathbf{H}_a^R$  will double in magnitude and will induce transitions  $|\chi_0\rangle \rightarrow |\chi_-\rangle$  and  $|\chi_0\rangle \rightarrow |\chi_+\rangle$  with some probability [45]. Because for the  $P$  and  $S$  pulse order in Fig. 2 the dark state  $|\chi_0\rangle$  is equal to state  $|1\rangle$  in the beginning and to state  $-|3\rangle$  in the end, then remaining in the dark state  $|\chi_0\rangle$  for the  $L$  handedness implies complete population

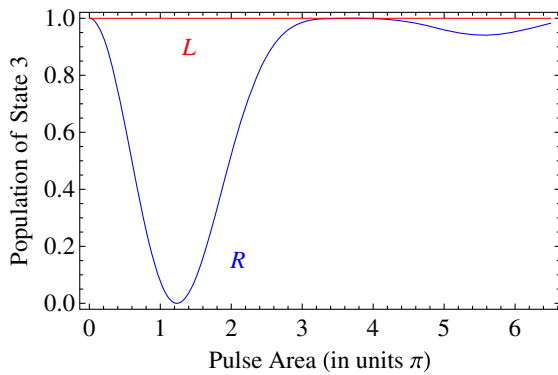


FIG. 3. Population  $P_3$  of state  $|3\rangle$  vs the pulse area  $A$  of the  $P$  and  $S$  couplings for Gaussian pulses with delay  $\tau = T$ , and the  $Q$  coupling is given by Eq. (6). The population  $P_3$  for  $L$  handedness is exactly equal to 1 due to the shortcut to adiabaticity, whereas it varies for  $R$  handedness due to the nonzero nonadiabatic coupling and approaches 1 as the pulse area  $A$  increases because the adiabaticity improves. The largest contrast between the signals occurs for  $A \approx 1.234\pi$ , where the  $R$  signal vanishes.

transfer from state  $|1\rangle$  to state  $|3\rangle$ . On the contrary, if the dark state  $|\chi_0\rangle$  is depleted due to the enhanced nonadiabatic coupling for the  $R$  handedness, then no population will be found in state  $|3\rangle$  in the end. Therefore, if the three-state system is initially in state  $|1\rangle$  then the different signs of the  $Q$  coupling for  $L$  and  $R$  handedness will map onto different population distributions at the end of the interaction: monitoring the population of state  $|3\rangle$  alone will tell us if the molecule is  $L$  or  $R$  handed.

It is important to note that, contrary to STIRAP [30], here the aim is *not* adiabatic evolution because in the adiabatic limit the nonadiabatic coupling ( $\propto \dot{\theta}$ ) will be suppressed by the large pulse areas and complete population transfer will take place for both  $L$  and  $R$  handedness, thereby rendering the difference in the coupling magnitudes irrelevant. Here it is crucial to have a significant nonadiabatic coupling  $\dot{\theta}(t)$ , so that the two enantiomers behave very differently. It turns out that this condition is fulfilled for small pulse areas (of the order of  $\pi$ ), which implies that the proposed method is faster than the earlier adiabatic scenarios.

*Maximum population contrast.*—From an experimental point of view, ideally, we want to have unit transition probability to state  $|3\rangle$  for one handedness ( $L$  in this example), and zero transition probability for the opposite handedness ( $R$  in this example). This would create a maximum contrast in the signals for the two enantiomers. The value 1 for the  $L$  handedness is guaranteed by the choice of Eq. (6). The value 0 for the  $R$  handedness can occur for a particular choice of the experimental parameters, as explained below.

For the commonly used Gaussian pulse shapes,  $\Omega_p(t) = \Omega_0 e^{-(t-\tau/2)^2/T^2}$  and  $\Omega_s(t) = \Omega_0 e^{-(t+\tau/2)^2/T^2}$  (delay  $\tau$  and width  $T$ ), the  $Q$  pulse is  $\Omega_q(t) = \pm 2(\tau/T) \text{sech}(2\tau t/T^2)$ . These three pulse shapes are shown in Fig. 2. For a fixed pulse delay  $\tau$ , complete population depletion of the adiabatic state  $|\chi_0\rangle$  takes place for a special value of the peak  $P$  and  $S$  Rabi frequency  $\Omega_0$ , or equivalently, for a special value of the  $P$  and  $S$  pulse area  $A = \Omega_0 T \sqrt{\pi}$ . For example, for  $\tau/T = 0.6, 0.8, 1.0,$  and  $1.2$ , these values are (derived numerically)  $A \approx 0.891\pi, 1.035\pi, 1.234\pi,$  and  $1.510\pi$ . For these pairs of pulse delays and pulse areas, and given the condition (6) for the  $Q$  coupling, the application of the  $P$ ,  $Q$ , and  $S$  pulses of Fig. 2 will result in complete population transfer  $|1\rangle \rightarrow |3\rangle$  for  $L$  handedness ( $P_3 = 1$ ), whereas zero population will reach state  $|3\rangle$  for the opposite  $R$  handedness ( $P_3 = 0$ ). Figure 3 illustrates these findings.

It is important to note that as long as the  $Q$  coupling has a relative phase of  $\pm\pi/2$  there will be a large difference between the magnitudes of the couplings for the  $L$  and  $R$  handedness, even if the condition (6) is not precisely fulfilled, and the population distribution (and the ensuing signals) will differ. Indeed, because at the point where  $P_3 = 0$  this population has a minimum, there is some interval of pulse area values wherein the population  $P_3$  is very small and the contrast is very high; see Fig. 3.

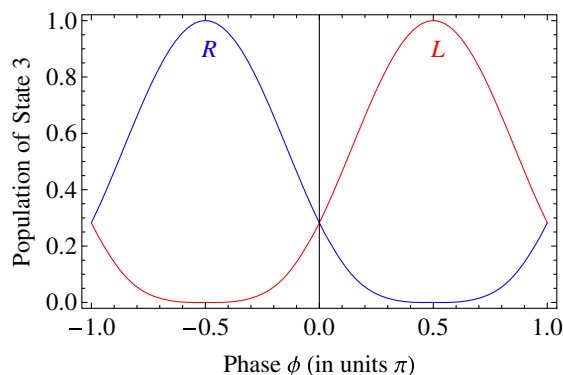


FIG. 4. Population  $P_3$  of state  $|3\rangle$  vs the phase  $\phi$  of the  $Q$  field for  $L$  and  $R$  handedness. The  $P$  and  $S$  pulses are Gaussian, with a delay  $\tau = T$  and pulse areas  $A = 1.234\pi$ . The  $Q$  coupling is given by Eq. (6). The largest contrast is obtained for  $\phi = \pm\pi/2$  when one of the populations is 1 and the other is 0. For  $\phi = 0$  and  $\pm\pi$ , the two enantiomers produce the same signal and the contrast vanishes.

However, condition (6) is still desirable for it delivers the highest contrast between the  $L$  and  $R$  signals.

Figure 4 shows the expected variations of the  $L$  and  $R$  signals from state  $|3\rangle$  versus the phase  $\phi$  of the  $Q$  field, which has been assumed to be  $\pi/2$  so far. For  $\phi = \pi/2$ , the  $L$  signal is 1 and the  $R$  signal is 0, as expected. Conversely, for  $\phi = -\pi/2$ , the  $L$  signal is 0 and the  $R$  signal is 1. As in Fig. 3, there are some ranges of phases around the perfect values  $\pm\pi/2$  wherein the contrast remains very high. For phase  $\phi = 0, \pm\pi$  the  $L$  and  $R$  signals are equal and the contrast vanishes completely: the enantiomers are indistinguishable.

So far we assumed Gaussian shapes for the  $P$  and  $S$  pulses. Our method is not restricted to these pulse shapes. Another example is presented in the Supplemental Material [46] for an exactly soluble analytic model, which allows us to derive the transition probability explicitly (see also Refs. [47–49]).

*Enantiomer detection and separation.*—For larger ensembles of molecules, the efficiency and contrast in the enantiomer-specific state transfer process could be measured through light-induced fluorescence (LIF) from molecules in state  $|3\rangle$ , while separation of the enantiomers could be achieved by applying a resonantly enhanced multiphoton ionization (REMPI) scheme to selectively ionize the enantiomer ending up in state  $|3\rangle$ , and by an electric field remove the ionized molecules. Together with the high efficiency in detecting single ions either by an electron-multiplier detector or an ion trap [50], the REMPI method furthermore enables the ultimate detection of a single specific enantiomer molecule. In case the original chirality of the neutral molecule is preserved after REMPI, the capture of this ion in an ion trap already containing a single laser cooled atomic ion, one can, actually, produce a single chiral molecular ion which is both trapped and cooled to low translational temperatures. In some cases,

one should even be able to produce the chiral molecule in a specific internal state by REMPI, as has been demonstrated with  $N_2^+$  [51]. This could enable novel studies of chemical processes and parity violation in chiral molecules [2,3].

The potential advantage of our scheme lies partly in its ability to address states more widely separate in energy, which makes state dependent ionization easier, partly in prospect of spatially very localized interactions through applying crossed laser beams. This is an asset when the goal is to create, trap, and conduct experiment with a single chiral molecular ion produced from an initial neutral molecule sample.

*Feasibility.*—Because of the shortcuts to adiabaticity approach, the pulse areas in our scheme are greatly reduced compared to the earlier adiabatic methods and are similar to methods using resonant  $\pi$  or  $\pi/2$  pulses. Therefore, our scheme can be implemented in all systems in which resonant  $\pi$  pulses have been implemented for chiral resolution. At the same time, our scheme is expected to be more robust to experimental errors, while delivering almost perfect enantiomer contrast. For example, a combination of resonant microwave and chirped rf fields has been used [34] on two of the transitions between three rotational levels to discriminate  $R$  carvone from  $S$  carvone by measuring the phase of the emitted microwave field on the third transition. This approach, termed microwave three-wave mixing, has been used also to distinguish (+) menthone and (–) menthone [36], and the enantiomers of 1,2-propanediol [32], 1,3-butanediol [33], and 4-carvo-menthenol [35]. The electric dipole moments of the three transitions in all these experiments are of the order of 1 Debye and the pulse durations are fractions of a microsecond, which allows the generation of the pulses required in our method with standard microwave generators.

Similar experimental conditions have been present in several recent experiments when all three transitions in a closed three-state system have been resonantly driven by microwave fields, resulting in control of the population distribution, as in our method. Chiral resolution was achieved with 1,2-propanediol in a buffer gas cell [40] as well as with menthone and carvone in supersonic beams [41]. A combination of closed-loop population transfer and three-wave mixing was used in cyclohexylmethanol [52]. We point out also a recent paper [53], which focusses at the design of cyclic three-level configurations in chiral molecules.

In the optical domain, several molecules have been discussed as a possible platform of all-optical chiral resolution by using optical transitions between vibrational levels. One of them is  $H_2D_2$  which is transiently chiral [27]. A promising candidate is 1,3-dimethylallene [54], wherein a closed three-level transition has been identified [29] with dipole moments in the range 0.005–0.065 Debye, which require infrared laser intensities of the order of  $10^5$ – $10^8$  W/cm<sup>2</sup> with nanosecond pulses. Such intensities should be fairly easily reachable by applying a pulsed

optical parametric oscillator system [55] injection seeded by a quantum cascade laser [56].

We also note recent studies of parity violation by using STIRAP between vibrational levels of chiral molecules. First spectroscopic investigations on two molecules—1,2 dithiine [57] and trisulfane [58]—prove promising. The respective vibrational transitions are suitable for the application of our method too, as it requires far less pulse areas than STIRAP.

The challenge of the multidimensional internal degrees of freedom associated with the usually complex structure of chiral molecules is envisioned to be handled to a large extent by applying either a supersonic jet source [59] or an ultracold buffer gas source [60], where a mixture (e.g., racemic) of the chiral molecule of interest is introduced. Both these sources will ensure a high probability of finding the chiral molecule in a specific low-lying state. With velocities of the molecules leaving these sources in the range 10–1000 m/s, and laser pulses in the nanosecond range, in a crossed-beam scenario, the molecules of interest will typically move less than 10  $\mu\text{m}$  in the molecular beam direction, and hence much less in the directions of the laser fields.

*Conclusions.*—This paper presented a method for efficient detection and separation of chiral molecules. The tool is a closed-loop three-state system driven by three resonant external fields. All three couplings are the same in magnitude but one of them ( $Q$ ) has a different sign for  $L$ - and  $R$ -handed molecules. By using a suitable pulse delay, as in the STIRAP process, suitable pulse areas, and a phase shift of  $\pi/2$  of the  $Q$  field, and using concepts from the shortcuts to adiabaticity method, one can map the sign difference in the  $Q$  couplings to different transition probabilities, and hence different populations, for the  $L$ - and  $R$ -handed molecules.

Because our method populates different states in the end of the process, in the case of larger ensembles (e.g., molecules in a cold supersonic beam) it allows the spatial separation of the  $L$ - and  $R$ -handed molecules, e.g., by REMPI in the presence of an electric field. The REMPI technique furthermore enables the detection of a single molecule of a particular enantiomer, and potentially constitutes the starting point for the production and investigation of a single molecular ion with a specific chirality.

The authors acknowledge useful discussions with Christiane Koch. N. V. V. acknowledges support from the European Commission's Horizon-2020 Flagship on Quantum Technologies Project No. 820314 (MicroQC). M. D. acknowledges support from the European Commission's FET Open TEQ, the Villum Foundation and the Sapere Aude Initiative from the Independent Research Fund Denmark.

[1] L. Pasteur, *Ann. Chim. Phys.* **24**, 442 (1848).

[2] M. Quack, *Angew. Chem., Int. Ed. Engl.* **41**, 4618 (2002).

- [3] M. Quack, J. Stohner, and M. Willeke, *Annu. Rev. Phys. Chem.* **59**, 741 (2008).
- [4] W. S. Knowles, *Angew. Chem., Int. Ed. Engl.* **41**, 1998 (2002).
- [5] *Chiral Separation Methods for Pharmaceutical and Biotechnological Products*, edited by S. Ahuja (John Wiley & Sons, New York, 2011).
- [6] *Comprehensive Chiroptical Spectroscopy: Instrumentation, Methodologies, and Theoretical Simulations*, edited by N. Berova, P. L. Polavarapu, K. Nakanishi, and R. W. Woody (Wiley, New York, 2012).
- [7] N. Berova and K. Nakanishi, *Circular Dichroism: Principles and Applications* (Wiley, New York, 2000).
- [8] L. A. Nafie, *Vibrational Optical Activity: Principles and Applications* (Wiley, Chichester, 2011).
- [9] L. A. Nafie, T. A. Keiderling, and P. J. Stephens, *J. Am. Chem. Soc.* **98**, 2715 (1976).
- [10] C. Lux, M. Wollenhaupt, T. Bolze, Q. Liang, J. Köhler, C. Sarpe, and T. Baumert, *Angew. Chem., Int. Ed. Engl.* **51**, 4755 (2012).
- [11] C. S. Lehmann, N. B. Ram, I. Powis, and M. H. M. Janssen, *J. Chem. Phys.* **139**, 234307 (2013).
- [12] R. E. Goetz, T. A. Isaev, B. Nikoobakht, R. Berger, and C. P. Koch, *J. Chem. Phys.* **146**, 024306 (2017).
- [13] L. D. Barron, *Molecular Light Scattering and Optical Activity* (Cambridge University Press, Cambridge, England, 2004).
- [14] A. Salam and W. J. Meath, *J. Chem. Phys.* **106**, 7865 (1997).
- [15] A. Salam and W. J. Meath, *Chem. Phys.* **228**, 115 (1998).
- [16] Y. Fujimura, L. González, K. Hoki, J. Manz, and Y. Ohtsuki, *Chem. Phys. Lett.* **306**, 1 (1999).
- [17] Y. Fujimura, L. González, K. Hoki, D. Kröner, J. Manz, and Y. Ohtsuki, *Angew. Chem., Int. Ed. Engl.* **39**, 4586 (2000).
- [18] K. Hoki, D. Kröner, and J. Manz, *Chem. Phys.* **267**, 59 (2001).
- [19] K. Hoki, L. González, and Y. Fujimura, *J. Chem. Phys.* **116**, 8799 (2002).
- [20] L. González, D. Kröner, and I. R. Solá, *J. Chem. Phys.* **115**, 2519 (2001).
- [21] D. Kröner, M. F. Shibl, and L. González, *Chem. Phys. Lett.* **372**, 242 (2003).
- [22] M. Shapiro, E. Frishman, and P. Brumer, *Phys. Rev. Lett.* **84**, 1669 (2000); **91**, 129902(E) (2003).
- [23] P. Brumer, E. Frishman, and M. Shapiro, *Phys. Rev. A* **65**, 015401 (2001).
- [24] D. Gerbasi, M. Shapiro, and P. Brumer, *J. Chem. Phys.* **115**, 5349 (2001).
- [25] E. Frishman, M. Shapiro, D. Gerbasi, and P. Brumer, *J. Chem. Phys.* **119**, 7237 (2003).
- [26] P. Král and M. Shapiro, *Phys. Rev. Lett.* **87**, 183002 (2001).
- [27] P. Král, I. Thanopoulos, M. Shapiro, and D. Cohen, *Phys. Rev. Lett.* **90**, 033001 (2003).
- [28] I. Thanopoulos, P. Krl, and M. Shapiro, *J. Chem. Phys.* **119**, 5105 (2003).
- [29] D. Gerbasi, P. Brumer, I. Thanopoulos, P. Král, and M. Shapiro, *J. Chem. Phys.* **120**, 11557 (2004).
- [30] N. V. Vitanov, A. A. Rangelov, B. W. Shore, and K. Bergmann, *Rev. Mod. Phys.* **89**, 015006 (2017).

- [31] S. R. Domingos, C. Perez, and M. Schnell, *Annu. Rev. Phys. Chem.* **69**, 499 (2018).
- [32] D. Patterson, M. Schnell, and J. M. Doyle, *Nature (London)* **497**, 475 (2013).
- [33] D. Patterson and J. M. Doyle, *Phys. Rev. Lett.* **111**, 023008 (2013).
- [34] V. A. Shubert, D. Schmitz, D. Patterson, J. M. Doyle, and M. Schnell, *Angew. Chem., Int. Ed. Engl.* **53**, 1152 (2014).
- [35] V. A. Shubert, D. Schmitz, C. Medcraft, A. Krin, D. Patterson, J. M. Doyle, and M. Schnell, *J. Chem. Phys.* **142**, 214201 (2015).
- [36] V. A. Shubert, D. Schmitz, C. Perez, C. Medcraft, A. Krin, S. R. Domingos, D. Patterson, and M. Schnell, *J. Phys. Chem. Lett.* **7**, 341 (2016).
- [37] G. G. Brown, B. C. Dian, K. O. Douglass, S. M. Geyer, S. T. Shipman, and B. H. Pate, *Rev. Sci. Instrum.* **79**, 053103 (2008).
- [38] B. G. Park and R. Field, *J. Chem. Phys.* **144**, 200901 (2016).
- [39] Y. Li and C. Bruder, *Phys. Rev. A* **77**, 015403 (2008).
- [40] S. Eibenberger, J. Doyle, and D. Patterson, *Phys. Rev. Lett.* **118**, 123002 (2017).
- [41] C. Perez, A. L. Steber, S. R. Domingos, A. Krin, D. Schmitz, and M. Schnell, *Angew. Chem.* **129**, 12686 (2017).
- [42] R. G. Unanyan, L. P. Yatsenko, K. Bergmann, and B. W. Shore, *Opt. Commun.* **139**, 48 (1997).
- [43] M. Demirplak and S. A. Rice, *J. Phys. Chem. A* **107**, 9937 (2003).
- [44] X. Chen, I. Lizuain, A. Ruschhaupt, D. Guéry-Odelin, and J. G. Muga, *Phys. Rev. Lett.* **105**, 123003 (2010).
- [45] We note that if we choose, instead,  $\Omega_q(t) = -2\dot{\theta}(t)$ , then the opposite will happen: the off-diagonal elements of  $\mathbf{H}_a^L$  will double in magnitude, while those of  $\mathbf{H}_a^R$  will vanish.
- [46] See Supplemental Material at <http://link.aps.org/supplemental/10.1103/PhysRevLett.122.173202> for an analytically soluble model of chiral detection.
- [47] N. V. Vitanov and S. Stenholm, *Phys. Rev. A* **55**, 648 (1997).
- [48] N. V. Vitanov and K.-A. Suominen, *Phys. Rev. A* **56**, R4377 (1997).
- [49] J. Randall, A. M. Lawrence, S. C. Webster, S. Weidt, N. V. Vitanov, and W. K. Hensinger, *Phys. Rev. A* **98**, 043414 (2018).
- [50] K. Højbjerg, D. Offenberg, C. Z. Bisgaard, H. Stapelfeldt, P. F. Staunum, A. Mortensen, and M. Drewsen, *Phys. Rev. A* **77**, 030702(R) (2008).
- [51] X. Tong, A. H. Winney, and S. Willitsch, *Phys. Rev. Lett.* **105**, 143001 (2010).
- [52] C. Perez, A. L. Steber, A. Krin, and M. Schnell, *J. Phys. Chem. Lett.* **9**, 4539 (2018).
- [53] C. Ye, Q. Zhang, and Y. Li, *Phys. Rev. A* **98**, 063401 (2018).
- [54] E. Dereţey, M. Shapiro, and P. Brumer, *J. Phys. Chem. A* **105**, 9509 (2001).
- [55] G. Mennerat and P. Kupecek, High-energy narrow-linewidth tunable source in the mid infrared, in *Trends in Optics and Photonics, Advanced Solid-State Lasers*, Vol. 19, edited by W. R. Bosenberg and M. M. Fejer (Optical Society of America, 1998), pp. 269–272, <https://www.osapublishing.org/abstract.cfm?uri=ASSL-1998-FC13>.
- [56] R. Maulini, D. A. Yarekha, J.-M. Bulliard, M. Giovannini, J. Faist, and E. Gini, *Opt. Lett.* **30**, 2584 (2005).
- [57] S. Albert, I. Bolotova, Z. Chen, C. Fabri, L. Horny, M. Quack, G. Seyfang, and D. Zindel, *Phys. Chem. Chem. Phys.* **18**, 21976 (2016).
- [58] S. Albert, I. Bolotova, Z. Chen, C. Fabri, M. Quack, G. Seyfang, and D. Zindel, *Phys. Chem. Chem. Phys.* **19**, 11738 (2017).
- [59] G. Scoles, *Atomic and Molecular Beam Methods* (Oxford University Press, New York, 1988).
- [60] N. R. Hutzler, H.-I. Lu, and J. M. Doyle, *Chem. Rev.* **112**, 4803 (2012).